

## Low-Field de Haas-van Alphen Effect in Copper

A. S. JOSEPH, A. C. THORSEN, E. GERTNER, AND L. E. VALBY  
*North American Aviation Science Center, Thousand Oaks, California*

(Received 28 February 1966)

Detailed studies of the de Haas-van Alphen (dHvA) effect in Cu single crystals have been carried out with a high-sensitivity torque magnetometer in steady fields up to 40 kG. The angular variations of all pertinent dHvA frequencies were determined to better than 0.1%. New frequencies, found near the  $\langle 100 \rangle$  directions, are attributable to noncentral extremal orbits on the belly portion of the Fermi surface. For each dHvA term observed in this study there existed orientations at which the amplitude of the fundamental vanishes as a result of the vanishing of the spin-splitting factor.

### INTRODUCTION

IN recent publications we reported on detailed de Haas-van Alphen (dHvA) effect studies of the Fermi surfaces of Ag<sup>1</sup> and Au.<sup>2</sup> Like Shoenberg's<sup>3</sup> earlier pulsed-field data, our own measurements exhibited good general accord with the model originally proposed by Pippard.<sup>4</sup> In addition to providing very high-accuracy determinations of the angular variations of all pertinent Fermi-surface segments, we reported evidence for the existence of noncentral extremal belly orbits. In this report we have, in a similar fashion, completed the study of the Fermi-surface segments in Cu. We find evidence for noncentral extremal belly orbits near the  $\langle 100 \rangle$  direction, but as in the case of Au such orbits appear to be absent near the  $\langle 111 \rangle$  direction. For each segment of the Fermi surface in Cu, there exist magnetic field directions at which the dHvA amplitude vanishes due to spin-splitting effects.<sup>5,6</sup>

### EXPERIMENTAL

The experimental details of the null-deflection torsion balance have been described fully in previous reports.<sup>1,7</sup> The experimental techniques were similar to those used in the cases of Ag and Au: changes in phase (defined as the ratio of  $F/H_0$ , where  $F$  is the dHvA frequency and  $H_0$  is the applied field) were monitored in a constant magnetic field as the field was rotated about the axis of suspension. This procedure leads to a very accurate determination of the relative change in frequency because each change of phase of the belly, for example, corresponds to a change in frequency of 0.01% at  $H \approx 40$  kG. The dominant errors in this type of measurement lie in the determination of the angle at which the phase was measured and in the absolute value of the

magnetic field. Typically, the error in reading the angle was about 0.05°. The error in the determination of the magnetic field, by a Rawson probe, was estimated to be about 0.2%. The dHvA frequencies were all reproducible to within 0.2%, although the absolute error was estimated to be approximately 0.5% in each case.

An unannealed copper crystal having a resistivity ratio of  $\approx 2700$  was grown by K. Garr of Atomics International. Two samples were spark cut in the form of cylinders (length  $\approx 0.140$  in. and diameter  $\approx 0.100$  in.) and annealed at 900°C for 24 h and brought back to room temperature at a rate of 30°C per hour. The samples were then mounted and oriented so that the magnetic field was located in the  $\{100\}$  and  $\{110\}$  symmetry planes to better than 1°. Annealing of the cut crystals was found to quadruple the amplitudes of the signals. A typical recording of the oscillations is shown in Fig. 1.

### RESULTS AND DISCUSSION

The angular variations of the belly ( $F_{B1}, F_{B2}$ ), the dog's bone ( $F_D$ ), the four-cornered rosette ( $F_R$ ), and the neck ( $F_N$ ) frequencies are shown in Figs. 2-7 and are tabulated in Tables I-V. (As in previous work,  $F_{B1}$  denotes the belly frequency arising from the *central* extremal cross section and  $F_{B2}$  the frequency arising from the *noncentral* cross section.) In all cases the angle  $\theta$  is measured from the  $\langle 100 \rangle$  axis in the  $\{110\}$

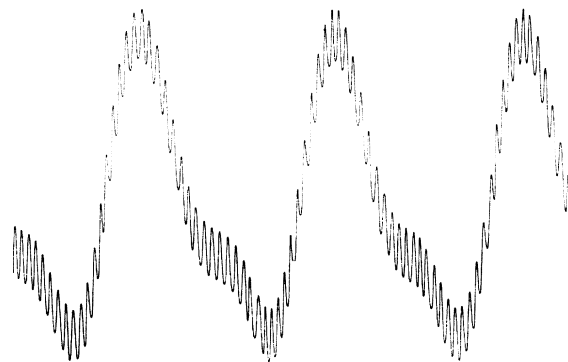


FIG. 1. A typical recording of torque versus  $H$  near the  $\langle 111 \rangle$  axis. The low frequencies are  $F_N$  and its second harmonic and the high frequency is  $F_{B1}$ .

<sup>1</sup> A. S. Joseph and A. C. Thorsen, Phys. Rev. 138, A1159 (1965).

<sup>2</sup> A. S. Joseph, A. C. Thorsen, and F. A. Blum, Phys. Rev. 140, A2046 (1965).

<sup>3</sup> D. Shoenberg, Phil. Trans. Roy. Soc. London A255, 85 (1962).

<sup>4</sup> A. B. Pippard, Phil. Trans. Roy. Soc. London A250, 325 (1957).

<sup>5</sup> I. M. Lifshitz and A. M. Kosevich, Zh. Eksperim. i Teor. Fiz. 29, 730 (1955) [English transl.: Soviet Phys.—JETP 2, 636 (1956)].

<sup>6</sup> M. Cohen and E. I. Blount, Phil. Mag. 5, 115 (1960).

<sup>7</sup> A. S. Joseph and A. C. Thorsen, Phys. Rev. 133, A1546 (1964), and references therein.

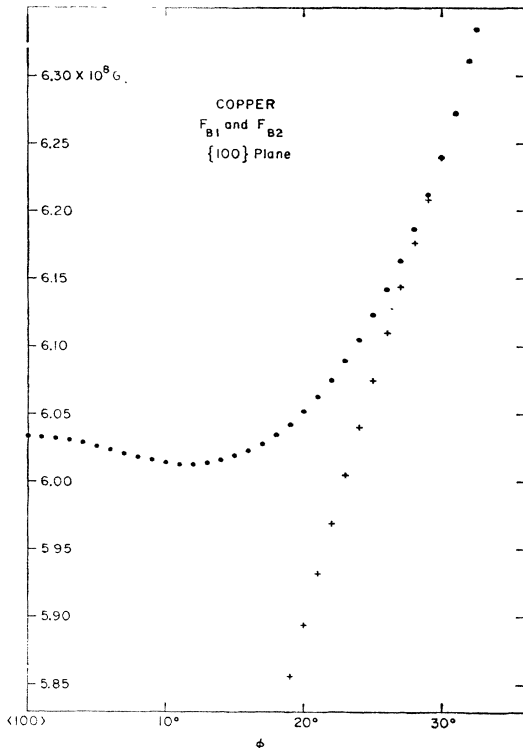


FIG. 2. Plots of the dHvA frequencies of the belly oscillations  $F_{B1}$  and  $F_{B2}$  in the  $\{100\}$  plane as functions of the angle  $\varphi$  between the field and the  $\langle 100 \rangle$  axis.

plane, and the angle  $\varphi$  is measured from the  $\langle 100 \rangle$  axis in the  $\{100\}$  plane. The absolute values of  $F_{B1}$ ,  $F_R$ , and  $F_D$  were obtained by counting 2000, 800, and 900 oscillations, respectively.  $F_N$  was obtained from the accurately known ratio  $F_{B1}/F_N$ , determined in a region near the  $\langle 111 \rangle$  axis where both oscillations were observed simultaneously. The absolute values of these frequencies agree with those of earlier work<sup>3</sup> to within 2% in all cases except that of  $F_N$  where the disagreement is 12%.

TABLE I.  $F_{B1}$ ,  $F_{B2}$ ,  $F_R$ , and  $F_D$  (in units of  $10^8$  gauss) in the  $\{100\}$  plane. The angle  $\varphi$  is measured from the  $\langle 100 \rangle$  axis.

$\varphi$	$F_{B1}$	$F_R$	$\varphi$	$F_{B1}$	$F_{B2}$	$\varphi$	$F_D$
0	6.0337	2.4751	17	6.0281		33.8	2.8223
1	6.0334	2.4767	18	6.0347		34	2.8056
2	6.0324	2.4816	19	6.0426	5.8558	35	2.7421
3	6.0308	2.4899	20	6.0520	5.8940	36	2.6932
4	6.0287	2.5018	21	6.0628	5.9316	37	2.6534
5	6.0262	2.5175	22	6.0753	5.9686	38	2.6201
6	6.0235	2.5373	23	6.0894	6.0050	39	2.5927
7	6.0208	2.5615	24	6.1052	6.0406	40	2.5702
8	6.0182	2.5908	25	6.1228	6.0756	41	2.5522
9	6.0160	2.6262	26	6.1422	6.1099	42	2.5382
10	6.0143	2.6697	27	6.1634	6.1437	43	2.5284
10.7		2.7062	28	6.1865	6.1766	44	2.5224
11	6.0133		29	6.2118	6.2086	45	2.5203
12	6.0134		30	6.2397	6.2397		
13	6.0141		31	6.2722			
14	6.0159		32	6.3114			
15	6.0188		32.5	6.3345			
16	6.0228		33				

TABLE II.  $F_{B1}$ ,  $F_{B2}$ , and  $F_R$  (in units of  $10^8$  gauss) in the  $\{110\}$  plane. The angle  $\theta$  is measured from the  $\langle 100 \rangle$  axis.

$\theta$	$F_{B1}$	$F_R$	$\theta$	$F_{B1}$	$F_{B2}$
0	6.0337	2.4751	14	5.9949	
1	6.0331	2.4768	15	5.9933	5.8290
2	6.0320	2.4817	16	...	5.8711
3	6.0302	2.4901	16.18	5.9928	..
4	6.0278	2.5024	17	5.9932	5.9069
5	6.0250	2.5189	18	5.9945	5.9366
6	6.0217	2.5400	19	5.9970	5.9610
7	6.0181	2.5674	20	6.0009	5.9808
8	6.0143	2.6042	21	6.0061	5.9971
8.8	...	2.6473	22	6.0132	6.0109
9	6.0104		23	6.0224	6.0224
10	6.0066		23.73	6.0309	6.0309
11	6.0030		24	6.0346	
12	5.9998		25	6.0507	
13	5.9970		25.58	6.0688	

The angular variations of  $F_{B1}$  are very similar to those of Ag and Au.  $F_{B1}$  has a minimum near the  $\langle 100 \rangle$  direction at  $\theta=16.2^\circ$  and  $\varphi=11^\circ$ . In the regions  $15^\circ \leq \theta \leq 23^\circ$ ,  $19^\circ \leq \varphi \leq 30^\circ$ , another frequency  $F_{B2}$  associated with a noncentral belly orbit is observed. It merges with  $F_{B1}$  at  $\theta=23^\circ$  and  $\varphi \cong 30.1^\circ$ . For lower  $\theta$  and  $\varphi$  it decreases more rapidly than  $F_{B1}$  and finally disappears at  $\theta=15^\circ$  and  $\varphi=19^\circ$ . The difference frequency  $F_{B1}-F_{B2}=F_C$ , which had a strong amplitude in Ag and Au, was barely visible in Cu. Near the  $\langle 111 \rangle$  direction, no oscillations were observed that could be associated with a difference frequency, which suggests,

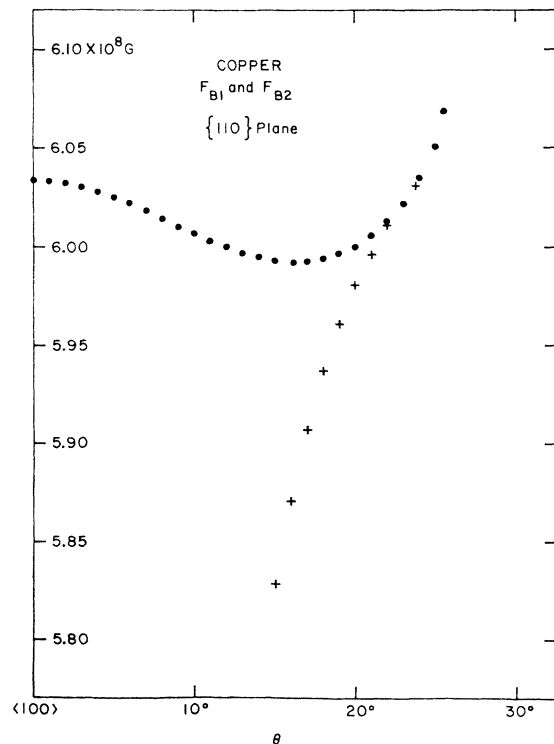


FIG. 3. Plots of the dHvA frequencies of the belly oscillations  $F_{B1}$  and  $F_{B2}$  in the  $\{110\}$  plane as functions of the angle  $\theta$  between the field and  $\langle 100 \rangle$  axis.

TABLE III.  $F_{B1}$  (in units of  $10^8$  gauss) in the  $\{110\}$  plane. The angle  $\theta$  is measured from the  $\langle 100 \rangle$  axis. The angle  $\theta = 54.75^\circ$  corresponds to  $H$  along the  $\langle 111 \rangle$  axis.

$\theta$	$F_{B1}$	$\theta$	$F_{B1}$
45	5.9700	59	5.8651
46	5.9380	60	5.8747
47	5.9157	61	5.8863
48	5.8978	62	5.8999
49	5.8829	63	5.9155
50	5.8710	64	5.9331
51	5.8618	65	5.9526
52	5.8548	66	5.9740
53	5.8501	67	5.9976
54	5.8475	68	6.0232
54.75	5.8468	69	6.0513
55	5.8469	70	6.0826
56	5.8484	71	6.1177
57	5.8520	72	6.1568
58	5.8575	72.3	6.1702

as in the case of Au, that only central belly orbits exist in this region. Figure 8 shows a plot of  $F_{B1}(\alpha)/F_{B1}(111)$  versus  $\alpha$  compared with the angular variation of the cross-sectional area of a cylinder ( $\alpha$  denotes an angle measured from the  $\langle 111 \rangle$  axis). It can be seen that  $F_{B1}(\alpha)$  varies more rapidly than that associated with a cylinder. This behavior indicates further

TABLE IV.  $F_D$  (in units of  $10^8$  gauss) in the  $\{110\}$  plane. The angle  $\theta$  is measured from the  $\langle 100 \rangle$  axis.

$\theta$	$F_D$
79.8	2.6253
80	2.6209
81	2.6003
82	2.5827
83	2.5676
84	2.5548
85	2.5441
86	2.5355
87	2.5289
88	2.5242
89	2.5215
90	2.5203

TABLE V.  $F_N$  (in units of  $10^7$  gauss) in the  $\{110\}$  plane. The angle  $\theta$  is measured from the  $\langle 100 \rangle$  axis.

$\theta$	$F_N$	$\theta$	$F_N$	$\theta$	$F_N$
28.9	3.9374	47	2.2626	65	2.3201
29	3.9026	48	2.2440	66	2.3494
30	3.6203	49	2.2283	67	2.3825
31	3.4099	50	2.2153	68	2.4200
32	3.2361	51	2.2050	69	2.4620
33	3.0902	52	2.1971	70	2.5095
34	2.9656	53	2.1920	71	2.5630
35	2.8601	54	2.1887	72	2.6223
36	2.7682	54.75	2.1872	73	2.6896
37	2.6873	55	2.1881	74	2.7684
38	2.6166	56	2.1901	75	2.8587
39	2.5542	57	2.1941	76	2.9620
40	2.4988	58	2.2006	77	3.0833
41	2.4509	59	2.2096	78	3.2265
42	2.4087	60	2.2212	79	3.3931
43	2.3714	61	2.2356	80	3.6016
44	2.3385	62	2.2524	81	3.8636
45	2.3096	63	2.2721	82	4.2026
46	2.2844	64	2.2945	83	4.6650

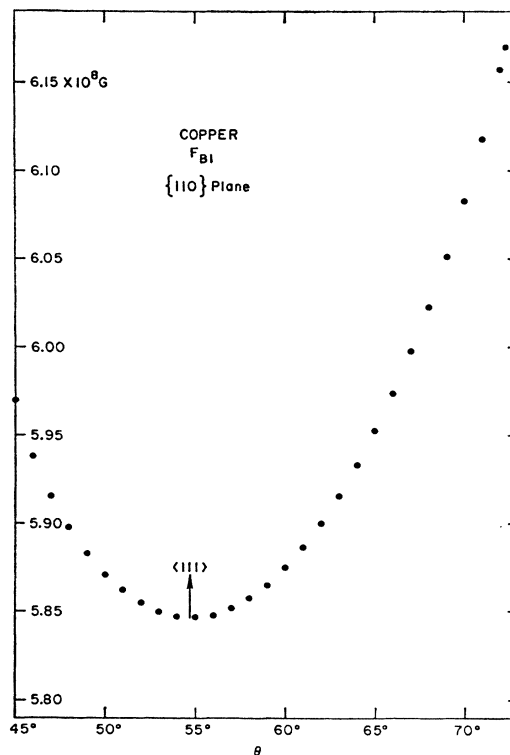


FIG. 4. Plot of the dHvA frequencies of the belly oscillations  $F_{B1}$  near the  $\langle 111 \rangle$  axis in the  $\{110\}$  plane as a function of  $\theta$ .

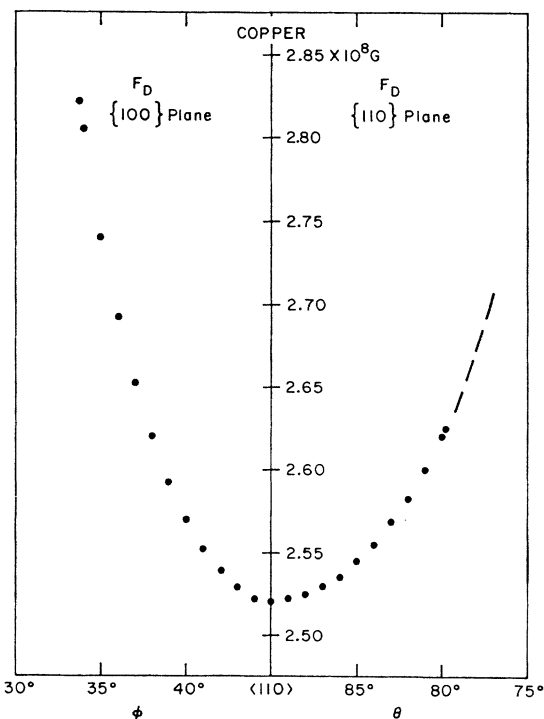


FIG. 5. Plots of the dHvA frequencies of the oscillations associated with the dog's bone in the  $\{100\}$  and  $\{110\}$  planes as functions of  $\phi$  and  $\theta$ . The dashed line shows the range over which  $F_D$  was observed but could not be accurately measured.

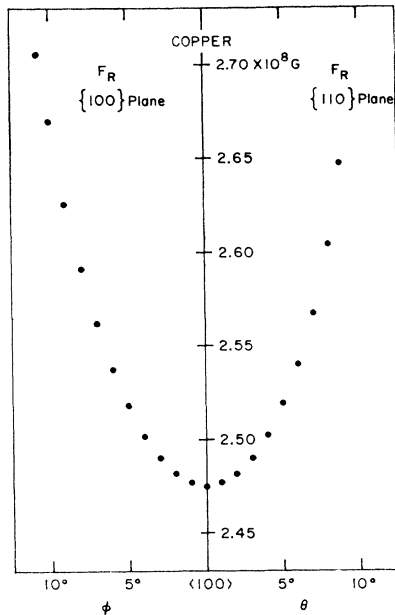


FIG. 6. Plots of the dHvA frequencies associated with the four-cornered rosette in the  $\{100\}$  and  $\{110\}$  planes as functions of  $\varphi$  and  $\theta$ .

that the central belly orbit in the  $\langle 111 \rangle$  direction is a minimum as a function of  $k_z$ , as in the case of Au. This is in agreement with Roaf's<sup>8</sup> analytical fit to Shoenberg's data.

The angular variations of  $F_D$  and  $F_R$  are shown in Figs. 5 and 6. The angular ranges over which they were observed are approximately as predicted by Roaf. In the  $\{110\}$  plane,  $F_D$  could be measured only through  $10^\circ$  with high accuracy. For  $\theta < 80^\circ$ , the fact that the phase of  $F_D$  was changing at approximately the same rate as the phase of  $F_N$  and that the amplitudes of the oscillations of  $F_N$  were much larger than those of  $F_D$  precluded the accurate determination of the dog's-bone phase. By observing the changes of phase as a function of magnetic field, however, and by differentiating the signal several times, we could detect  $F_D$  as far as  $\theta = 77^\circ$ . The extrapolated dashed line in Fig. 6 denotes the region where the oscillations associated with  $F_D$  could be detected.

$F_N$  was studied over the entire angular range in the  $\{110\}$  plane and could be fitted approximately to the formula

$$F_N(111)/F_N(\alpha) = (\cos\alpha)[1 - (m_t/m_l)\tan^2\alpha]^{1/2}, \quad (1)$$

for  $m_t/m_l = 2.54 \pm 0.10$ . The angle  $\alpha$  is measured from the  $\langle 111 \rangle$  axis. From earlier measurements<sup>9,10</sup>  $m_t$ , the transverse effective mass of the neck, was found to be  $(0.46 \pm 0.02)m_0$  and hence,  $m_l = (0.18 \pm 0.02)m_0$ . In

keeping with the crystal symmetry (and contrary to the approximate formula above), there is a slight asymmetry in the neck frequency in this plane,  $F_N$  having a value  $\sim 2.4\%$  higher for  $\theta = 32.75^\circ$  than at  $\theta = 76.75^\circ$ . The cylindrical sample whose axis lies along the  $[110]$  direction, which was used for the  $[110]$  suspension, was tilted  $30^\circ$  about the  $[1\bar{1}1]$  axis for an investigation of the possible existence of large anisotropy in the topology of the neck. We found that in this off-symmetry plane  $F_N$  is nearly symmetrical about the  $[1\bar{1}1]$  axis and also fits the theoretical formula above with the same value of the parameter  $m_t/m_l$ . There thus appear to be no large asymmetries that would indicate a strong deformation of the neck from circular cross section.

### THE AMPLITUDE OF THE OSCILLATIONS AND THE SPIN-SPLITTING FACTOR

In earlier reports, we discussed the vanishing of the amplitude of the dHvA oscillations due to the  $180^\circ$  phase shift between spin-up and spin-down Landau levels. For the electronic  $g$  factor equal to 2, this condition occurs when  $m^* = 0.5m_0, 1.5m_0$ , etc. In Fig. 9, we show the torque as a function of  $\theta$ , which is indicative of the angular dependence of the phase of the neck oscillations. Near  $\theta = 68.1^\circ$ , the amplitude of the fundamental frequency  $F_N$  goes to zero and reverses its phase as shown by the arrows, while the second har-

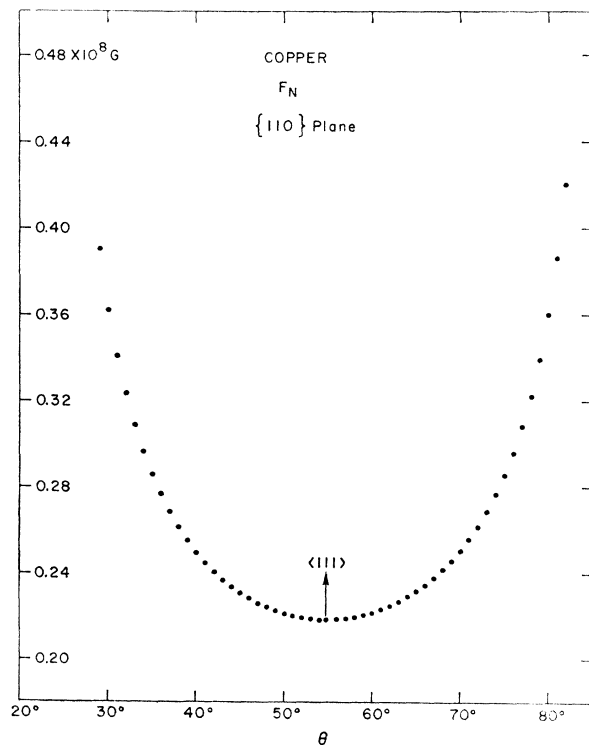


FIG. 7. Plot of the dHvA frequencies associated with the neck in the  $\{110\}$  plane as a function of  $\theta$ .

<sup>8</sup> D. J. Roaf, Phil. Trans. Roy. Soc. London **A255**, 135 (1962).

<sup>9</sup> A. S. Joseph and A. C. Thorsen, Phys. Rev. **134**, A979 (1964).

<sup>10</sup> J. F. Koch, R. A. Stradling, and A. F. Kip, Phys. Rev. **133**, A240 (1964).

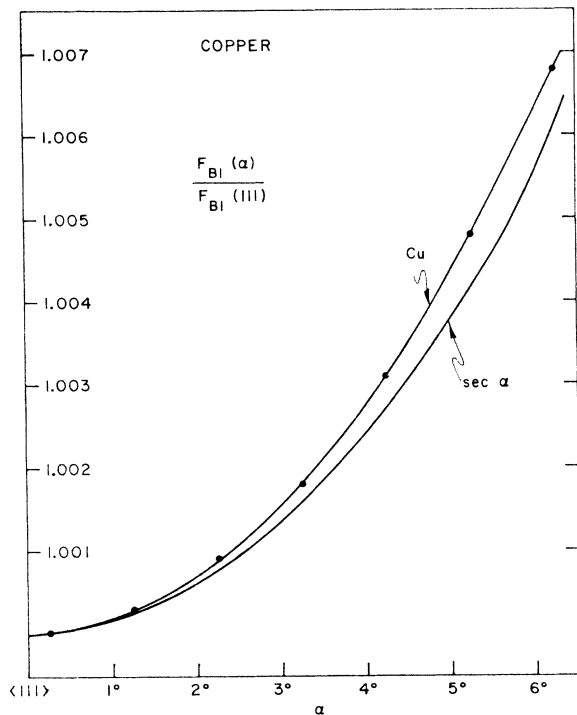


FIG. 8. Plots of the ratio  $F_B(\alpha)/F_B(111)$  versus angle from the  $\langle 111 \rangle$  axis compared to the variation expected for a cylindrical surface ( $\sec \alpha$ ).

monic reaches a maximum amplitude. From the temperature dependence of the amplitude of the second harmonic at this angle, a "harmonic effective mass" of  $(0.98 \pm 0.03)m_0$  was deduced, which is twice the effective mass of the fundamental,<sup>9,10</sup> in complete accord with the theory.<sup>5</sup> This corresponds to  $g=2.0$  for the neck orbit. Recent electron spin resonance experiments<sup>11</sup> by Schultz and Latham yielded a value of  $g=2.031 \pm 0.003$ , although the resonance experiments do not single out a particular orbit.

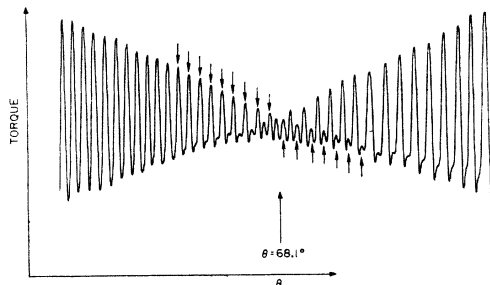


FIG. 9. Torque versus  $\theta$  near  $\theta=68^\circ$  at constant magnetic field. The oscillations represent the change of phase of  $F_N$ . At  $\theta=68.1^\circ$  the amplitude of the fundamental frequency  $F_N$  vanishes while the amplitude of its second harmonic becomes maximum. The arrows indicate the phase reversal as the oscillations go through  $\theta=68.1^\circ$ .

<sup>11</sup> Sheldon Schultz and Clancy Latham, Phys. Rev. Letters 15, 148 (1965).

For each Fermi-surface segment in Cu, field orientations were found at which the amplitude vanished due to the vanishing of the spin-splitting factor. In Table VI, we tabulate the angles at which this happens, and we compare, from the data of Koch, Stradling, and Kip,<sup>10</sup> with the angles at which the cyclotron masses have the values  $1.5m_0$  or  $0.5m_0$ . We find fair agreement. Several

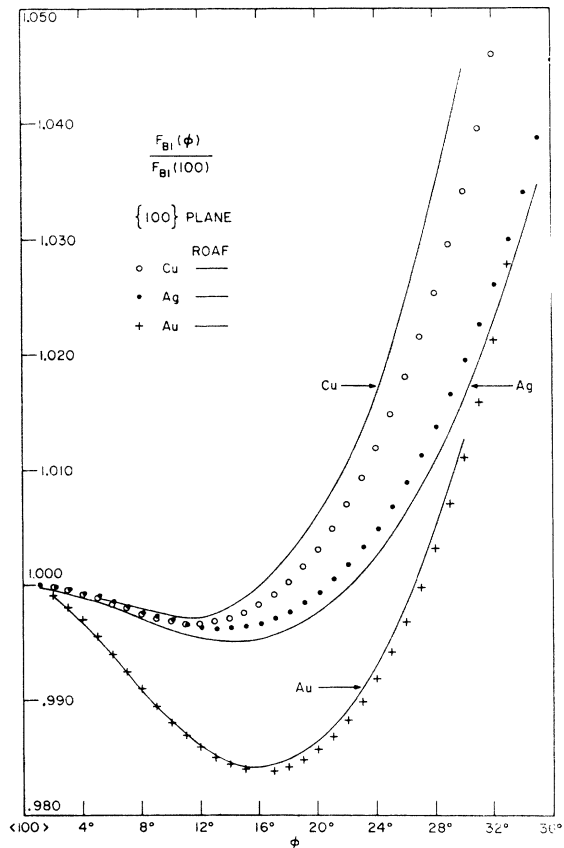


FIG. 10. Plots showing the relative variations of  $F_{B1}$  near the  $\langle 100 \rangle$  axis in the  $\{100\}$  plane for Cu, Ag, and Au. All the frequencies at  $\langle 100 \rangle$  are normalized to unity, including Roaf's analytical curves, denoted by solid lines.

mass determinations were made in the  $\langle 100 \rangle$  plane yielding the following values ( $\pm 5\%$ ):

$$m_D^*(\varphi=41^\circ)=1.37m_0, \quad m_R^*(\varphi=2^\circ)=1.34m_0, \\ M^*_B(\varphi=30.1^\circ)=1.52m_0.$$

These large values of effective mass undoubtedly play a major role in determining the amplitudes of the dHvA oscillations in Cu. The resistivity ratio in Cu was at least five times larger than that in Ag and yet the signal was several times weaker. One explanation for the small amplitudes of  $F_B$ ,  $F_R$ , and  $F_D$  is that their effective mass through most angular ranges varies from 1.3 to 1.6, whereas in Ag the average effective mass associated with these frequencies is almost  $1.0m_0$ . As an indication of the effect of this mass difference on

TABLE VI. Angles at which the amplitudes of the dHvA oscillations vanished compared with angles at which the cyclotron-mass data of Koch, Stradling, and Kip<sup>a</sup> show values of  $1.5m_0$  for  $F_B$ ,  $F_D$ , and  $F_R$  and  $0.5m_0$  for  $F_N$ .

(100) plane	This experiment	Koch <i>et al.</i>
$F_{B1}$	$\varphi \cong 27^\circ$	
$F_R$	$\varphi = 7.2^\circ$	
$F_D$	$\varphi = 36.8^\circ$	
(110) plane		
$F_{B1}$	$\theta = 23.8^\circ$	$24^\circ$ (extrapolated)
	$63.3^\circ$	$67^\circ$
	$48.3^\circ$	$45^\circ$ (extrapolated)
$F_R$	$\theta = 6.8^\circ$	$8^\circ$
$F_D$		$13^\circ$ (extrapolated)
$F_N$	$\theta = 41.7^\circ$	$42^\circ$
	$68.1^\circ$	$67^\circ$

<sup>a</sup> See Ref. 10.

the amplitudes, we have calculated from the theoretical formula<sup>5</sup> the ratio of the amplitudes for two identical Fermi-surface segments having masses of  $1.0m_0$  and  $1.4m_0$ . The amplitude of the oscillations for a mass of  $1.0m_0$  is approximately a factor of 80 larger than that for a mass of  $1.4m_0$ . It is thus reasonable to expect that in Cu a much higher resistivity ratio is needed to give dHvA amplitudes comparable to those of Ag.

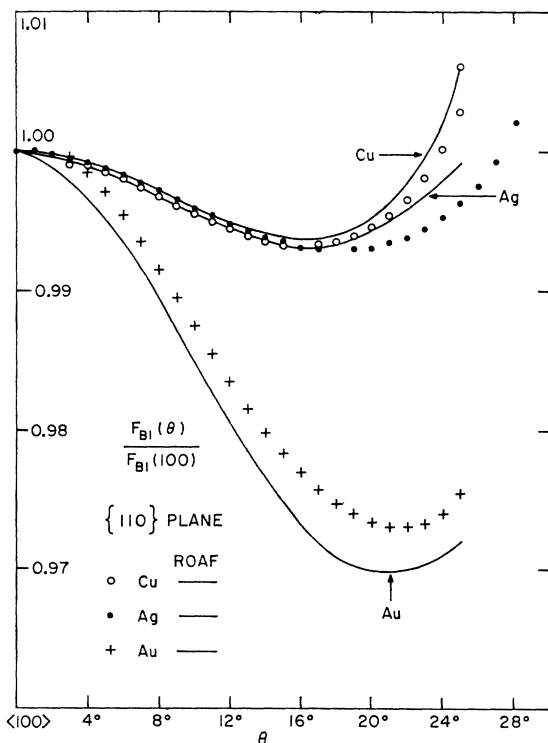


FIG. 11. Plots showing the relative variations of  $F_{B1}$  near the  $\langle 100 \rangle$  axis in the  $\{110\}$  plane for Cu, Ag, and Au. The frequencies, including Roaf's analytical curves, are normalized to unity along the  $\langle 100 \rangle$  axis.

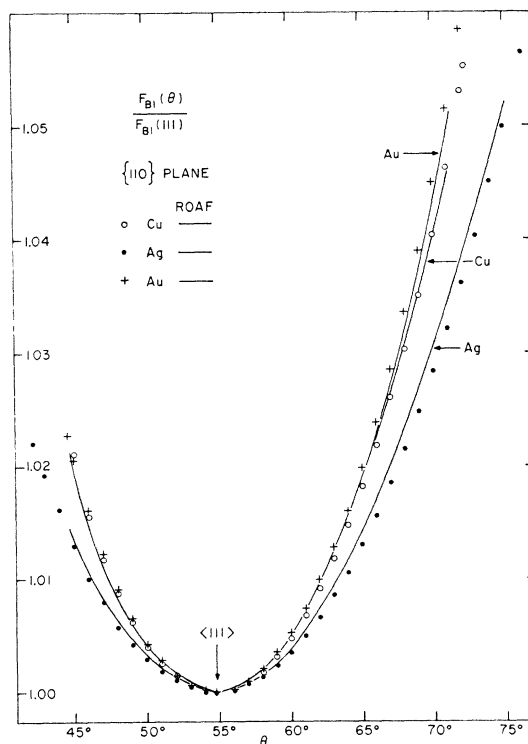


FIG. 12. Plots showing the relative variations of  $F_{B1}$  near the  $\langle 111 \rangle$  axis in the  $\{110\}$  plane for Cu, Ag, and Au. The frequencies are normalized to unity along the  $\langle 111 \rangle$  axis. The solid lines denote Roaf's analytical curves.

### CONCLUSIONS: Cu, Ag, AND Au

As found by Shoenberg and Roaf, the topologies of the Fermi surfaces in the noble metals are very similar. They differ only in fine structure, and the purpose of this series of investigations has been to study these fine features.

A convenient way of comparing the variations in cross-sectional areas of the noble metals is indicated in Figs. 10, 11, and 12. In these figures, the belly frequencies are normalized to unity along the  $\langle 100 \rangle$  and  $\langle 111 \rangle$  axes. It is apparent from Figs. 10 and 11 that the relative variation of frequency with angle near the  $\langle 100 \rangle$  axis is rather greater for Au than for Cu and Ag, the latter two having very similar behavior. The rather small change of frequency with angle near the  $\langle 100 \rangle$  axis for Cu and Ag suggests that the Fermi surfaces in these metals are much more spherical than that of Au. In Fig. 12, the relative variation of frequencies with angle near the  $\langle 111 \rangle$  axis indicates that the Fermi surfaces of all three metals deviate rapidly from sphericity, although the variation in Ag is less than that in either Cu or Au. The solid curves in Figs. 10–12 are the values computed by Roaf normalized to the present work along the  $\langle 100 \rangle$  and  $\langle 111 \rangle$  axes. In all cases, the agreement is within 1%.

As mentioned in earlier reports,  $F_N$  can be associated

with a surface having a shape of a hyperboloid of one sheet (with circular cross sections). Such a surface would be symmetrical about the  $\langle 111 \rangle$  axis. Strictly speaking,  $F_N$  is somewhat asymmetric, increasing slightly faster toward the  $\langle 100 \rangle$  axis than toward the  $\langle 110 \rangle$  axis. For an angle of approximately  $22^\circ$  on either side of the  $\langle 111 \rangle$  axis in the  $\{110\}$  plane, the percentage difference in  $F_N$  is  $\sim 0.4\%$ ,  $0.8\%$ , and  $2.4\%$  for Ag, Au, and Cu, respectively.

The  $g$  factor was estimated for the orbit associated with the neck in a region where the spin-splitting factor vanishes. For both Cu and Ag,  $g \approx 2.0$ , whereas in the

case of Au an estimated value of  $1.70 \pm 0.06$  was obtained. Such a difference in  $g$  may indicate a large spin-orbit coupling in Au as compared with Cu and Ag.

#### ACKNOWLEDGMENTS

We wish to thank K. Garr for growing the copper crystal, and M. Hiller for annealing the samples. We also thank D. Swarthout for his assistance in orienting the samples. A critical review of the manuscript by T. G. Berlincourt is appreciated.

## Least-Squares Determination of the Elastic Constants of Antimony and Bismuth

ALEXANDER DE BRETTEVILLE, JR.

*Institute for Exploratory Research, U. S. Army Electronics Command, Fort Monmouth, New Jersey*

AND

E. RICHARD COHEN

*North American Aviation Science Center, Thousand Oaks, California*

AND

ARTHUR D. BALLATO AND IRVING N. GREENBERG

*Electronic Components Laboratory and Institute for Exploratory Research,  
U. S. Army Electronics Command, Fort Monmouth, New Jersey*

AND

SEYMOUR EPSTEIN

*Electronic Components Laboratory, U. S. Army Electronics Command, Fort Monmouth, New Jersey*

(Received 28 September 1965; revised manuscript received 8 April 1966)

A least-squares determination of the elastic stiffness constants of antimony (using the data of Epstein and de Bretteville) and bismuth (using the data of Eckstein, Lawson, and Reneker) at room temperature was made by one of us (ERC). In the previous determination of the elastic constants of antimony and bismuth certain errors were not considered. They are considered in this paper. The antimony constants are:  $c_{11} = 101.3 \pm 1.6$ ;  $c_{13} = 29.2 \pm 2.2$ ;  $c_{33} = 45.0 \pm 1.5$ ;  $c_{44} = 39.3 \pm 0.7$ ;  $c_{14} = 20.9 \pm 0.4$ ;  $c_{66} = 33.4 \pm 0.6$ ; and  $c_{12} = 34.5 \pm 2.0$  all in units of  $10^{10}$  dyn  $\text{cm}^{-2}$ . The bismuth constants in the same units are:  $c_{11} = 63.7 \pm 0.2$ ;  $c_{13} = 24.7 \pm 0.2$ ;  $c_{33} = 38.2 \pm 0.2$ ;  $c_{44} = 11.23 \pm 0.04$ ;  $c_{66} = 19.41 \pm 0.06$ ;  $c_{12} = 24.9 \pm 0.2$ ;  $c_{14} = 7.17 \pm 0.04$ .

#### INTRODUCTION

THE earlier paper of Epstein and de Bretteville on ultrasonic velocity measurements in antimony and bismuth at room temperature did not include a least-squares determination, in depth, of the elastic constants of these crystals.<sup>1</sup> Since the number of wave velocities measured for different propagation and polarization directions was larger than the number of elastic moduli for these crystals, such a determination would increase the accuracy of the computed values of the elastic constants. The least-squares determination is presented in this paper along with an analysis of the

sources of experimental error and the final best values of the elastic constants of antimony and bismuth. The data for bismuth were taken from Eckstein, Lawson, and Reneker.<sup>2</sup>

#### VELOCITY ERRORS AND CORRECTIONS

The errors in measuring the echo time using the rf pulse-echo technique, in regard to the antimony measurement, are: (1) the uncertainty of measuring from the crest of one wave in one echo train (11 periods for shear and 20 periods for longitudinal waves) to the crest of the corresponding cycle in an adjacent train;

<sup>1</sup> S. Epstein and A. de Bretteville, Jr., Phys. Rev. **138**, A771 (1965).

<sup>2</sup> Y. Eckstein, A. W. Lawson, and D. H. Reneker, J. Appl. Phys. **31**, 1535 (1960).